JOURNAL OF GUIDANCE, CONTROL, AND DYNAMICS
Vol. 27, No. 1, January–February 2004

Decentralized Scheme for Spacecraft Formation Flying via the Virtual Structure Approach

Wei Ren and Randal W. Beard
Brigham Young University, Provo, Utah 84602

Built on the combined strength of decentralized control and the recently introduced virtual structure approach, a decentralized formation scheme for spacecraft formation flying is presented. Following a decentralized coordination architecture via the virtual structure approach, decentralized formation control strategies are introduced, which are appropriate when a large number of spacecraft are involved and/or stringent interspacecraft communication limitations are exerted. The effectiveness of the proposed control strategies is demonstrated through simulation results.

I. Introduction

THE concept of formation control has been studied extensively in the literature with application to the coordination of multiple robots,[1–10] unmanned air vehicles,[11] autonomous underwater vehicles,[12] satellites,[13,14] aircraft,[15] and spacecraft.[16–20] There are several advantages to using formations of multiple vehicles. These include increased feasibility, accuracy, robustness, flexibility, cost, energy efficiency, and probability of success. For example, sometimes large awkward objects cannot be moved efficiently by a single robot so that multiple robots must be used. Also the probability of success will be improved if multiple vehicles are used to carry out a mission, for example, multiple UAVs are assigned to a certain target[21] or multiple AUVs are used to search an underwater object.[12] In spacecraft formation-flying applications using multiple microspacecraft instead of a monolithic spacecraft can reduce the mission cost and improve system robustness and accuracy.[17]

Various strategies and approaches have been proposed for formation control. These approaches can be roughly categorized as leader-following, behavioral, and virtual structure approaches, to name a few. In the leader-following approach some agents are designated as leaders, whereas others are designated as followers. The leaders track predefined trajectories, and the followers track transformed versions of the states of their nearest neighbors according to given schemes. In the behavioral approach the control action for each agent is defined by a weighted average of the control corresponding to each desired behavior for the agent. In the virtual structure approach the entire formation is treated as a single rigid body. The virtual structure can evolve as a whole in a given direction with some given orientation and maintain a rigid geometric relationship among multiple agents. Similar ideas to the virtual structure approach include the perceptive reference frame proposed in Ref. 13 and the virtual leader proposed in Ref. 22.

There are numerous studies on the leader-following approach. In Ref. 1 nearest neighbor tracking strategies are used to control a fleet of autonomous mobile robots moving in formation. In Ref. 16 various schemes and explicit control laws for formation keeping and relative attitude alignment are derived for the coordination and control of multiple microspacecraft. Although the leader-following approach is easy to understand and implement, there are limitations. For example, the leader is a single point of failure for the formation. In addition, there is no explicit feedback from the followers to the leader: if the follower is perturbed by some disturbances, the formation cannot be maintained.

As an alternative to leader-following, the virtual structure approach was proposed in Ref. 3 to acquire high-precision formation control for mobile robots. In Ref. 23 the virtual structure approach is

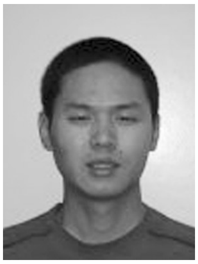

Wei Ren received the B.S. degree in electrical engineering from Hohai University, Nanjing, People's Republic of China, in 1997 and M.S. degree in electrical engineering from Tongji University, Shanghai, People's Republic of China, in 2000. He is currently working toward his Ph.D. degree in the Department of Electrical and Computer Engineering at Brigham Young University, Provo, Utah. His research interests include coordinated control of multiple vehicles, nonlinear control, and robotics.

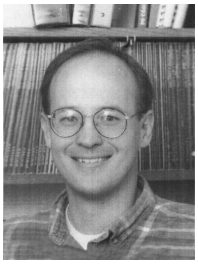

Randal W. Beard received the B.S. degree in electrical engineering from the University of Utah, Salt Lake City, in 1991; and the M.S. degree in electrical engineering in 1993, the M.S. degree in mathematics in 1994, and the Ph.D. degree in electrical engineering in 1995 from Rensselaer Polytechnic Institute, Troy, New York. Since 1996, he has been with the Electrical and Computer Engineering Department at Brigham Young University, Provo, Utah, where he is currently an Associate Professor. In 1997 and 1998, he was a Summer Faculty Fellow at the Jet Propulsion Laboratory, California Institute of Technology, Pasadena, California. His research interests include coordinated control of multiple vehicle systems and applications of control to autonomous vehicles. Member AIAA.

Received 10 October 2002; revision received 19 June 2003; accepted for publication 8 July 2003.

applied to the spacecraft interferometry problem, where formation maneuvers are easily prescribed, but no formation feedback is included from spacecraft to the virtual structure. In Ref. 10 a Lyapunov formation function is used to define a formation error, and formation feedback is incorporated to the virtual leaders through parameterized trajectories. In Ref. 24 the virtual structure approach is used to perform elementary formation maneuvers for mobile robots, where group feedback is incorporated from the followers to the virtual structure to improve group stability and robustness. Also in Ref. 25, following the idea of Ref. 24, formation feedback is applied to spacecraft formation-flying scenario via the virtual structure approach. One advantage of the virtual structure approach is that it is easy to prescribe the behavior for the group. Another advantage is that the virtual structure can maintain tight formation during maneuvers. The main disadvantage of the current virtual structure implementation is that it is centralized, which results in a single point of failure for the whole system.

The behavioral approach is a decentralized implementation and can achieve more flexibility, reliability, and robustness than centralized implementations. In Ref. 2 the behavioral approach is applied to formation keeping for mobile robots, where control strategies are derived by averaging several competing behaviors. In Ref. 26 several behavioral strategies are presented for formation maneuvers of groups of mobile robots, where a bidirectional ring topology is used to reduce the communication overhead for the whole system, and formation patterns are also defined to achieve a sequence of maneuvers. In Ref. 27 the behavioral approach is used to maintain attitude alignment among a group of spacecraft. An advantage of the behavioral approach is that explicit formation feedback is included through the communication between neighbors. Unfortunately, the behavioral approach is hard to analyze mathematically. Based on the way the formation patterns are defined in Ref. 26, the behavioral approach has limited application in directing rotational maneuvers for the group. In addition, the behavioral approach has limited ability for precise formation keeping, that is, the group cannot maintain formation very well during maneuvers.

Motivated by the advantages and disadvantages of each approach just discussed, a framework that is precise, reliable, and easy to implement needs to be constructed to achieve the following characteristics. First, the framework should be decentralized when a large number of agents are involved in the formation and/or there are stringent limitations on intervehicle communications. Second, formation feedback should be included in the framework to improve group robustness. Third, the group maneuvers should be easy to prescribe and direct in the framework. Finally, the framework should guarantee high precision for maintaining the formation during maneuvers. The purpose of this paper is to propose a solution that can achieve the benefits of each approach just discussed while overcoming their limitations. The main contribution of this paper is to apply the virtual structure approach in a decentralized scheme so that both the benefits of the virtual structure approach and the decentralized scheme can be achieved simultaneously. In this paper each spacecraft in the formation instantiates a local copy of the coordination vector in the virtual structure framework. The local instantiation of the coordination vector in each spacecraft is then synchronized by communication with its neighbors using a bidirectional ring topology.

The paper is organized as follows. In Sec. II, we introduce preliminary notation and definitions for spacecraft formation control. In Sec. III, we propose a new decentralized architecture via the virtual structure approach based on previous work on centralized architectures and decentralized control. In Sec. IV, we propose decentralized formation control strategies for each virtual structure instantiation and each spacecraft. In Sec. V, we demonstrate the effectiveness of our approach via a simulation study. Finally, in Sec. VI we offer some concluding remarks.

II. Problem Statement

In this section we introduce some preliminary notation and properties for spacecraft formation flying including reference frames, unit quaternions, desired states for each spacecraft, and spacecraft dynamics.

A. Reference Frames

Three coordinate frames are used in this paper. Reference frame $\mathcal{F}_0$ is used as an inertial frame. Reference frame $\mathcal{F}_F$ is fixed at the virtual center of the formation, that is, the virtual structure, as a formation frame. Reference frame $\mathcal{F}_i$ is embedded at the center of mass of each spacecraft as a body frame, which rotates with the spacecraft and represents its orientation. Given any vector $\boldsymbol{p}$, the representation of $\boldsymbol{p}$ in terms of its components in $\mathcal{F}_0$, $\mathcal{F}_F$, and $\mathcal{F}_i$ are represented by $[\boldsymbol{p}]_0$, $[\boldsymbol{p}]_F$, and $[\boldsymbol{p}]_i$, respectively.

Let the direction cosine matrix C_{ab} denote the orientation of the frame $\mathcal{F}_a$ with respect to $\mathcal{F}_b$, then $[\boldsymbol{p}]_a = C_{ab}[\boldsymbol{p}]_b$, where $[\boldsymbol{p}]_a$ and $[\boldsymbol{p}]_b$ are the coordinate representations of vector $\boldsymbol{p}$ in $\mathcal{F}_a$ and $\mathcal{F}_b$, respectively.

B. Unit Quaternions

Unit quaternions (see Ref. 28) are used to represent the attitude of rigid bodies in this paper. A unit quaternion is defined as $\boldsymbol{q} = [\hat{\boldsymbol{q}}^T, \bar{q}]^T$, where $\hat{\boldsymbol{q}} = \boldsymbol{a} \cdot \sin(\phi/2)$ and $\bar{q} = \cos(\phi/2)$. In this notation $\boldsymbol{a}$ is a unit vector in the direction of rotation with a coordinate representation $[a_1, a_2, a_3]^T$, called the eigenaxis, and ϕ is the rotation angle about $\boldsymbol{a}$, called the Euler angle. By definition, a unit quaternion is subject to the constraint that $\boldsymbol{q}^T\boldsymbol{q} = 1$. A unit quaternion is not unique because $\boldsymbol{q}$ and $-\boldsymbol{q}$ represent the same attitude. However, uniqueness can be achieved by restricting ϕ to the range $0 \le \phi \le \pi$ so that $\bar{q} \ge 0$ (Ref. 29). In the remainder of the paper, we assume that $\bar{q} \ge 0$.

The product of two unit quaternions $\boldsymbol{p}$ and $\boldsymbol{q}$ is defined by

$$\boldsymbol{qp} = \begin{bmatrix} \bar{q}\hat{\boldsymbol{p}} + \bar{p}\hat{\boldsymbol{q}} + \hat{\boldsymbol{q}} \times \hat{\boldsymbol{p}} \\ \bar{q}\bar{p} - \hat{\boldsymbol{q}}^T\hat{\boldsymbol{p}} \end{bmatrix}$$

which is also a unit quaternion. The conjugate of the unit quaternion $\boldsymbol{q}$ is defined by $\boldsymbol{q}^* = [-\hat{\boldsymbol{q}}^T, \bar{q}]^T$. The conjugate of $\boldsymbol{qp}$ is given by $(\boldsymbol{qp})^* = \boldsymbol{p}^*\boldsymbol{q}^*$. The multiplicative identity quaternion is denoted by $\mathbf{1} = [0, 0, 0, 1]^T$, where $\boldsymbol{qq}^* = \boldsymbol{q}^*\boldsymbol{q} = \mathbf{1}$ and $\boldsymbol{q}\mathbf{1} = \mathbf{1}\boldsymbol{q} = \boldsymbol{q}$. Suppose that $\boldsymbol{q}^d$ and $\boldsymbol{q}$ represent the desired and actual attitude respectively, then the attitude error is given by $\boldsymbol{q}_e = \boldsymbol{q}^{d*}\boldsymbol{q} = [\hat{\boldsymbol{q}}_e^T, \bar{q}_e]^T$, which represents the attitude of the actual reference frame $\mathcal{F}$ with respect to the desired reference frame $\mathcal{F}^d$.

The relationship between the rotation matrix C_{ab} and the unit quaternion $\boldsymbol{q}$ is given by

$$C_{ab} = (2\bar{q}^2 - 1)I + 2\hat{\boldsymbol{q}}\hat{\boldsymbol{q}}^T - 2\bar{q}\hat{\boldsymbol{q}}^\times$$

where $\boldsymbol{q}$ represents the attitude of $\mathcal{F}_a$ with respect to $\mathcal{F}_b$ (Ref. 28).

Given a vector $\boldsymbol{v}$ with coordinate representation $[v_1, v_2, v_3]^T$, the cross-product operator is denoted by[30]

$$\boldsymbol{v}^\times = \begin{bmatrix} 0 & -v_3 & v_2 \\ v_3 & 0 & -v_1 \\ -v_2 & v_1 & 0 \end{bmatrix}$$

which represents the fact that $\boldsymbol{v} \times \boldsymbol{w} = \boldsymbol{v}^\times\boldsymbol{w}$. Also $\Omega(\boldsymbol{v})$ is defined as

$$\Omega(\boldsymbol{v}) = \begin{bmatrix} -\boldsymbol{v}^\times & \boldsymbol{v} \\ -\boldsymbol{v}^T & 0 \end{bmatrix}$$

C. Desired States for Each Spacecraft

In the virtual structure approach the desired formation is treated as a single structure called the virtual structure with formation frame $\mathcal{F}_F$ located at its virtual center of mass to represent its configuration. The virtual structure then has position $\boldsymbol{r}_F$, velocity $\boldsymbol{v}_F$, attitude $\boldsymbol{q}_F$, and angular velocity $\boldsymbol{\omega}_F$ relative to $\mathcal{F}_0$.

Let $\boldsymbol{r}_i$, $\boldsymbol{v}_i$, $\boldsymbol{q}_i$, and $\boldsymbol{\omega}_i$ represent the position, velocity, attitude, and angular velocity of the ith spacecraft relative to the inertial frame $\mathcal{F}_0$. Similarly, let $\boldsymbol{r}_{\mathrm{iF}}$, $\boldsymbol{v}_{\mathrm{iF}}$, $\boldsymbol{q}_{\mathrm{iF}}$, and $\boldsymbol{\omega}_{\mathrm{iF}}$ represent the position, velocity, attitude, and angular velocity of the ith spacecraft relative to the formation frame $\mathcal{F}_F$. A superscript d is also used to represent the corresponding desired state of each spacecraft relative to either $\mathcal{F}_0$ or $\mathcal{F}_F$.

Conceptually, we can think that place holders corresponding to each spacecraft are embedded in the virtual structure to represent the desired position and attitude for each spacecraft. As the virtual structure as a whole evolves in time, the place holders trace out trajectories for each corresponding spacecraft to track. As a result, the actual states of the ith place holder represent the desired states of the ith spacecraft. With $\mathcal{F}_F$ as a reference frame, these states can be denoted by $\boldsymbol{r}_{\mathrm{iF}}^d$, $\boldsymbol{q}_{\mathrm{iF}}^d$, $\boldsymbol{v}_{\mathrm{iF}}^d$, and $\boldsymbol{\omega}_{\mathrm{iF}}^d$.

Generally, $\boldsymbol{r}_{\mathrm{iF}}^d$, $\boldsymbol{q}_{\mathrm{iF}}^d$, $\boldsymbol{v}_{\mathrm{iF}}^d$, and $\boldsymbol{\omega}_{\mathrm{iF}}^d$ can vary with time, which means the desired formation shape is time varying. However, if we are concerned with formation maneuvers that preserve the overall formation shape, that is, each place holder needs to preserve fixed relative position and orientation in the virtual structure, $\boldsymbol{r}_{\mathrm{iF}}^d$ and $\boldsymbol{q}_{\mathrm{iF}}^d$ should be constant and $\boldsymbol{v}_{\mathrm{iF}}^d$ and $\boldsymbol{\omega}_{\mathrm{iF}}^d$ should be zero. This requirement can be loosened to make the formation shape more flexible by allowing the place holders to expand or contract while still keeping fixed relative orientation. We will focus on this scenario. Of course, the approach here can be readily extended to the general case.

Let $\boldsymbol{\lambda}_F = [\lambda_1, \lambda_2, \lambda_3]$, where the components represent the expansion/contraction rates of the virtual structure along each $\mathcal{F}_F$ axis. The state of the virtual structure can be defined as $\boldsymbol{\xi} = [\boldsymbol{r}_F^T, \boldsymbol{v}_F^T, \boldsymbol{q}_F^T, \boldsymbol{\omega}_F^T, \boldsymbol{\lambda}_F^T, \dot{\boldsymbol{\lambda}}_F^T]^T$. If each spacecraft has knowledge of $\boldsymbol{\xi}$, and its own desired position and orientation with respect to the virtual structure, then formation keeping is transformed into an individual tracking problem. Therefore, the vector $\boldsymbol{\xi}$ represents the minimum amount of information needed by each spacecraft to coordinate its motion with the group. Motivated by this reasoning, we will call $\boldsymbol{\xi}$ the coordination vector.

Given $\boldsymbol{\xi}$, the desired states for the ith spacecraft are given by

$$\left[\boldsymbol{r}_i^d\right]_0 = [\boldsymbol{r}_F]_0 + C_{0F}\Lambda\left[\boldsymbol{r}_{\mathrm{iF}}^d\right]_F$$

$$\left[\boldsymbol{v}_i^d\right]_0 = [\boldsymbol{v}_F]_0 + C_{0F}\dot{\Lambda}\left[\boldsymbol{r}_{\mathrm{iF}}^d\right]_F + [\boldsymbol{\omega}_F]_0 \times \left(C_{0F}\Lambda\left[\boldsymbol{r}_{\mathrm{iF}}^d\right]_F\right)$$

$$\left[\boldsymbol{q}_i^d\right]_0 = [\boldsymbol{q}_F]_0\left[\boldsymbol{q}_{\mathrm{iF}}^d\right]_F, \qquad \left[\boldsymbol{\omega}_i^d\right]_0 = [\boldsymbol{\omega}_F]_0 \tag{1}$$

where $C_{0F}(\boldsymbol{q}_F)$ is the rotation matrix of the frame $\mathcal{F}_0$ with respect to $\mathcal{F}_F$ and $\Lambda = \mathrm{diag}(\boldsymbol{\lambda}_F)$. Note that unlike the constant desired states $\boldsymbol{r}_{\mathrm{iF}}^d$, $\boldsymbol{v}_{\mathrm{iF}}^d$, $\boldsymbol{q}_{\mathrm{iF}}^d$, and $\boldsymbol{\omega}_{\mathrm{iF}}^d$ relative to $\mathcal{F}_F$, the desired states $\boldsymbol{r}_i^d$, $\boldsymbol{v}_i^d$, $\boldsymbol{q}_i^d$, and $\boldsymbol{\omega}_i^d$ relative to $\mathcal{F}_0$ are time varying because $\boldsymbol{\xi}$ is time varying. The evolution equations of the desired states are given by

$$\left[\dot{\boldsymbol{r}}_i^d\right]_0 = \left[\boldsymbol{v}_i^d\right]_0$$

$$\left[\dot{\boldsymbol{v}}_i^d\right]_0 = [\dot{\boldsymbol{v}}_F]_0 + 2[\boldsymbol{\omega}_F]_0 \times \left(C_{0F}\dot{\Lambda}\left[\boldsymbol{r}_{\mathrm{iF}}^d\right]_F\right) + C_{0F}\ddot{\Lambda}\left[\boldsymbol{r}_{\mathrm{iF}}^d\right]_F + [\dot{\boldsymbol{\omega}}_F]_0 \times \left(C_{0F}\Lambda\left[\boldsymbol{r}_{\mathrm{iF}}^d\right]_F\right)$$

$$\left[\dot{\boldsymbol{q}}_i^d\right]_0 = [\dot{\boldsymbol{q}}_F]_0\left[\boldsymbol{q}_{\mathrm{iF}}^d\right]_F, \qquad \left[\dot{\boldsymbol{\omega}}_i^d\right]_0 = [\dot{\boldsymbol{\omega}}_F]_0 \tag{2}$$

D. Spacecraft Dynamics

The translational dynamics of each spacecraft relative to $\mathcal{F}_0$ are

$$\frac{\mathrm{d}\boldsymbol{r}_i}{\mathrm{d}t_0} = \boldsymbol{v}_i, \qquad m_i\frac{\mathrm{d}\boldsymbol{v}_i}{\mathrm{d}t_0} = \boldsymbol{f}_i \tag{3}$$

where m_i and $\boldsymbol{f}_i$ are the mass and control force associated with the ith spacecraft, respectively.

The rotational dynamics of each spacecraft relative to $\mathcal{F}_0$ (Ref. 16) are

$$\frac{\mathrm{d}\hat{\boldsymbol{q}}_i}{\mathrm{d}t_0} = -\frac{1}{2}\boldsymbol{\omega}_i \times \hat{\boldsymbol{q}}_i + \frac{1}{2}\bar{q}_i\boldsymbol{\omega}_i, \qquad \frac{\mathrm{d}\bar{q}_i}{\mathrm{d}t_0} = -\frac{1}{2}\boldsymbol{\omega}_i \cdot \hat{\boldsymbol{q}}_i$$

$$J_i\frac{\mathrm{d}\boldsymbol{\omega}_i}{\mathrm{d}t_0} = -\boldsymbol{\omega}_i \times (J_i\boldsymbol{\omega}_i) + \boldsymbol{\tau}_i \tag{4}$$

where J_i and $\boldsymbol{\tau}_i$ are inertia tensor and control torque associated with the ith spacecraft, respectively.

III. Decentralized Architecture via the Virtual Structure Approach

In this section we propose a decentralized architecture for spacecraft formation flying via the virtual structure approach. To demonstrate the salient features of our decentralized scheme, we first introduce previous work on centralized architectures via the virtual structure approach and previous work on general decentralized control architectures.

A. Previous Work on Centralized Architectures

Reference 23 introduced the general centralized coordination architecture shown in Fig. 1, which is based on the virtual structure approach.

The system $\boldsymbol{G}$ is a discrete event supervisor, which evolves a series of formation patterns by outputting its current formation pattern $\boldsymbol{y}_G$. The system $\boldsymbol{F}$ is the formation control module, which produces and broadcasts the coordination vector $\boldsymbol{\xi}$. The system $\boldsymbol{K}_i$ is the local spacecraft controller for the ith spacecraft, which receives the coordination vector $\boldsymbol{\xi}$ from the formation control module, converts $\boldsymbol{\xi}$ to the desired states for the ith spacecraft, and then controls the actual state for the ith spacecraft to track its desired state. The system $\boldsymbol{S}_i$ is the ith spacecraft, with control input $\boldsymbol{u}_i$ representing control force and torque and output $\boldsymbol{y}_i$ representing the measurable outputs from the ith spacecraft. In this centralized scheme $\boldsymbol{G}$ and $\boldsymbol{F}$ are implemented at a centralized location (e.g., spacecraft #1), and then the coordination vector $\boldsymbol{\xi}$ is broadcast to the local controllers of the other spacecraft. There is formation feedback from each local spacecraft controller to the formation control module $\boldsymbol{F}$ through the performance measure z_i. Also there is formation feedback from $\boldsymbol{F}$ to $\boldsymbol{G}$ through the performance measure z_F (Ref. 23).

The strength of this centralized scheme is that formation algorithms are fairly easy to realize. The weakness is that heavy communication and computation burden is concentrated on the centralized location, which may degrade the overall system performance. Also the centralized location results in a single point of failure for the whole system.

B. Previous Work on Decentralized Control

In Ref. 14 a decentralized architecture is proposed for autonomous establishment and maintenance of satellite formations, where each satellite only processes local measurement information and transmission vectors from the other nodes so that a local Kalman filter can be implemented to obtain a local control. It is also shown that the decentralized framework generates a neighboring optimal control if the planned maneuvers and trajectories are themselves optimal.

In Ref. 26 a decentralized control is implemented using a bidirectional ring topology, where each robot only needs position information of its two neighbors. A formation pattern is defined to be a set composed of the desired locations for each robot, that is,

$$P = \left\{h_1^d, \ldots, h_N^d\right\}$$

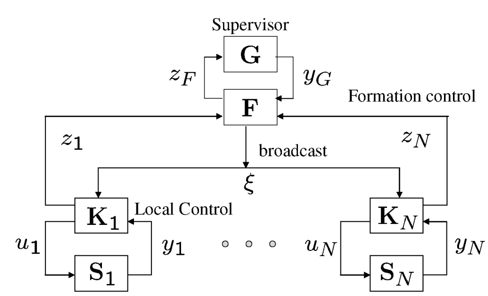

Fig. 1 Centralized architecture based on the virtual structure approach.

where N is the number of mobile robots in the formation. Two competing objectives are considered. The first objective is to move the robots to their final destinations. The second objective is to maintain formation during the transition. The goal of the control law for each robot is to drive the total tracking error and formation error of the group to zero. Similarly, in Ref. 27 three objectives are considered for the synchronized multiple-spacecraft rotation problem. The first objective is to rotate each spacecraft to zero attitude error. The second objective is to maintain formation throughout the maneuver. The third objective is to rotate the spacecraft about a defined axis of rotation.

C. Decentralized Architecture

In this paper, instead of using a set of desired locations for each agent as a formation pattern, we take advantage of the virtual structure approach to define the formation pattern by $P = \boldsymbol{\xi}^d$, where $\boldsymbol{\xi}^d = [\boldsymbol{r}_F^{d^T}, \boldsymbol{v}_F^{d^T}, \boldsymbol{q}_F^{d^T}, \boldsymbol{\omega}_F^{d^T}, \boldsymbol{\lambda}_F^{d^T}, \dot{\boldsymbol{\lambda}}_F^{d^T}]^T$ is the desired constant coordination vector representing the desired states of the virtual structure. We will assume piecewise rigid formations, which implies that $\boldsymbol{v}_F^d = \boldsymbol{\omega}_F^d = \dot{\boldsymbol{\lambda}}_F^d \equiv 0$. By specifying the formation pattern for the group, the movements of each spacecraft can be completely defined. Through a sequence of formation patterns $P^{(k)} = \boldsymbol{\xi}^{d(k)}$, $k = 1, \ldots, K$, the group can achieve a class of formation maneuver goals. In Ref. 26 the formation pattern is defined in such a way that each vehicle only knows its final location in the formation although its trajectory throughout the maneuver is not specified. Here the formation pattern is defined such that each spacecraft will track a trajectory specified by the state of the virtual structure while preserving a certain formation shape. From this point of view, collision avoidance is handled more efficiently than in Ref. 26.

In our decentralized architecture each spacecraft in the formation instantiates a local copy of the coordination vector. We use $\boldsymbol{\xi}_i = [\boldsymbol{r}_{\mathrm{Fi}}^T, \boldsymbol{v}_{\mathrm{Fi}}^T, \boldsymbol{q}_{\mathrm{Fi}}^T, \boldsymbol{\omega}_{\mathrm{Fi}}^T, \boldsymbol{\lambda}_{\mathrm{Fi}}^T, \dot{\boldsymbol{\lambda}}_{\mathrm{Fi}}^T]^T$ to represent the coordination vector instantiated in the ith spacecraft corresponding to the coordination vector $\boldsymbol{\xi}$ defined in Sec. II.C. A bidirectional ring topology is used to communicate the coordination vector instantiation instead of the position or attitude information among each spacecraft. A decentralized architecture via the virtual structure approach is shown in Fig. 2.

In this case, instead of implementing the discrete event supervisor and formation control module at a centralized location, each spacecraft has a local copy of the discrete event supervisor $\boldsymbol{G}$ and formation control module $\boldsymbol{F}$, denoted by $\boldsymbol{G}_i$ and $\boldsymbol{F}_i$ for the ith spacecraft respectively. As in Fig. 1, $\boldsymbol{K}_i$ and $\boldsymbol{S}_i$ represent the ith local spacecraft controller and the ith spacecraft, respectively.

Before the group maneuver starts, a sequence of formation patterns has been preset in each discrete event supervisor $\boldsymbol{G}_i$. The goal of $\boldsymbol{G}_i$ is to transition through the sequence of formation patterns so that a class of group maneuver goals can be accomplished sequentially. Certain mechanisms need to be applied to coordinate and synchronize the group starting time, for example, simple semaphores.

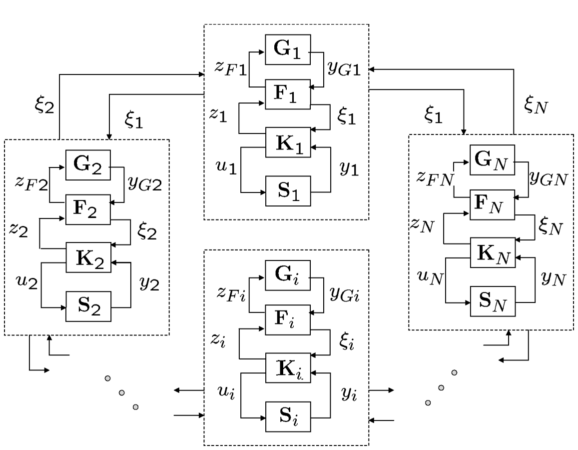

Fig. 2 Decentralized architecture via the virtual structure approach.

When the group maneuver starts, each discrete event supervisor $\boldsymbol{G}_i$ outputs the current formation pattern $\boldsymbol{y}_{\mathrm{Gi}} = \boldsymbol{\xi}^{d(1)}$, to the formation control module $\boldsymbol{F}_i$. Each formation control module $\boldsymbol{F}_i$ implements a coordination vector instantiation $\boldsymbol{\xi}_i$. The goal of $\boldsymbol{F}_i$ is to evolve $\boldsymbol{\xi}_i$ to its current desired formation pattern $\boldsymbol{\xi}^{d(k)}$ and synchronize $\boldsymbol{\xi}_i$ with coordination vector instantiations implemented on other spacecraft. Here we use a bidirectional ring topology, which means that the coordination vector $\boldsymbol{\xi}_i$ instantiated in the ith spacecraft is synchronized with its two neighbors, that is, instantiations $\boldsymbol{\xi}_{i-1}$ and $\boldsymbol{\xi}_{i+1}$ implemented in the $(i-1)$th and the $(i+1)$th spacecraft, respectively. Communications between the ith spacecraft and the $(i-1)$th and $(i+1)$th spacecraft need to be established to transmit and receive the coordination vector instantiations. The formation control module $\boldsymbol{F}_i$ then sends its coordination vector instantiation $\boldsymbol{\xi}_i$ to the local spacecraft controller $\boldsymbol{K}_i$. Based on $\boldsymbol{\xi}_i$, the local controller $\boldsymbol{K}_i$ can derive the desired states and the corresponding derivatives for the ith spacecraft from Eqs. (1) and (2). A local controller $\boldsymbol{K}_i$ is designed to guarantee that the ith spacecraft tracks its desired states asymptotically. Formation feedback is also included from the ith spacecraft controller $\boldsymbol{K}_i$ to the ith formation control module $\boldsymbol{F}_i$ through the performance measure z_i, indicating the ith spacecraft's tracking performance. Accordingly, as we will see in Sec. IV, the control law for $\boldsymbol{\xi}_i$ implemented in $\boldsymbol{F}_i$ depends on the performance measure z_i, the current desired formation pattern $\boldsymbol{y}_{\mathrm{Gi}} = \boldsymbol{\xi}^{d(k)}$, and the corresponding coordination vector instantiations $\boldsymbol{\xi}_{i-1}$ and $\boldsymbol{\xi}_{i+1}$ from the ith spacecraft's neighbors. Of course, formation feedback can also be included from other spacecraft to the ith formation control module $\boldsymbol{F}_i$ at the cost of additional communication. Formation feedback from the ith formation control module $\boldsymbol{F}_i$ to the ith discrete event supervisor $\boldsymbol{G}_i$ is also included through the performance measure z_{Fi}, which indicates how far the ith instantiation $\boldsymbol{\xi}_i$ is from its current maneuver goal $\boldsymbol{\xi}^{d(k)}$ and synchronization performance between $\boldsymbol{\xi}_i$ and its neighbors. Like the coordination and synchronization of the first group maneuver starting time, similar mechanisms can be applied to indicate the accomplishment of the current formation pattern and coordinate and synchronize the starting time for the next formation pattern among spacecraft. Then the same procedure just described repeats so that a sequence of formation patterns can be achieved.

Compared with the architecture in Ref. 14, which is based on a fully interconnected network, the architecture proposed here imposes fewer communication requirements. Even if the compression of data transmission is realized in Ref. 14, each vehicle still needs extensive data transmitted from all the other vehicles, which causes additional intervehicle communications especially when a large number of vehicles are involved. The architecture proposed here only requires communication between adjacent neighbors during the maneuver.

The communication requirement for each spacecraft during the maneuver can be estimated as follows. We know that $\boldsymbol{r}_{\mathrm{Fi}}$, $\boldsymbol{v}_{\mathrm{Fi}}$, $\boldsymbol{\omega}_{\mathrm{Fi}}$, $\boldsymbol{\lambda}_{\mathrm{Fi}}$, and $\dot{\boldsymbol{\lambda}}_{\mathrm{Fi}}$ all have three components and $\boldsymbol{q}_{\mathrm{Fi}}$ has four components. Thus the coordination vector $\boldsymbol{\xi}_i$ has 19 components. Assume that each component is encoded as B bits and the sample rate of the system is given by L Hz. By communicating with its two adjacent neighbors, the required bandwidth for each spacecraft can be estimated as $38BL$ bits/s. Note that this is the case when group translation, group rotation, and group expansion/contraction are all involved. If only one group maneuver is involved, the bandwidth can be further reduced to almost one-third of the preceding bandwidth estimate.

Compared to its centralized alternative, there is no master in the loop, and each spacecraft evolves in a parallel manner so that a single point of failure existing in any centralized implementation can be eliminated, and the total system performance will not degrade catastrophically under failure. As a result, the decentralized implementation offers more flexibility, reliability, and robustness than the corresponding centralized alternative. The weakness is that each local instantiation must be synchronized, which accounts for additional complexity and intervehicle communications. Because of the ring topology and the implementation of the coordination vector, information exchange among spacecraft can be reduced in the preceding decentralized architecture. Therefore, this weakness can be somewhat mitigated although the disadvantage of increased intervehicle communication requirements is a typical concern for decentralized systems. Of course, there might exist discrepancies between the starting time of each instantiation of the coordination vector dynamics. This starting time discrepancy can be mitigated through the control law for each coordination vector, which will synchronize neighboring coordination vector instantiations. Also, there might exist a time delay when neighboring spacecraft exchange information. This issue is not modeled in the preceding decentralized architecture and needs to be addressed in future work.

IV. Decentralized Formation Control Strategies

Two major tasks need to be carried out in the decentralized formation control scheme via the virtual structure approach. One is to propose suitable control laws for each spacecraft to track its desired states defined by the virtual structure. The other is to control and synchronize each virtual structure instantiation to achieve the desired formation patterns in a decentralized manner. In Secs. IV.A and IV.B, we present control strategies for each spacecraft and each virtual structure instantiation, respectively. In Sec. IV.C, we provide convergence analysis for the system composed of the coupled dynamics of N spacecraft and N coordination vector instantiations.

A. Formation Control Strategies for Each Spacecraft

For the ith spacecraft, define $\boldsymbol{X}_i=[\boldsymbol{r}_i^T,\boldsymbol{v}_i^T,\boldsymbol{q}_i^T,\boldsymbol{\omega}_i^T]^T$ and $\boldsymbol{X}_i^d=[\boldsymbol{r}_i^{d^T},\boldsymbol{v}_i^{d^T},\boldsymbol{q}_i^{d^T},\boldsymbol{\omega}_i^{d^T}]^T$ as the actual state and desired state, respectively. Define $\tilde{\boldsymbol{X}}_i=\boldsymbol{X}_i-\boldsymbol{X}_i^d=[\tilde{\boldsymbol{r}}_i^T,\tilde{\boldsymbol{v}}_i^T,\tilde{\boldsymbol{q}}_i^T,\tilde{\boldsymbol{\omega}}_i^T]^T$ as the error state for ith spacecraft.

We know that the desired states for each spacecraft also satisfy the translational and rotational dynamics (3) and (4) respectively, that is,

$$\frac{\mathrm{d}\boldsymbol{r}_i^d}{\mathrm{d}t_0}=\boldsymbol{v}_i^d,\qquad m_i\frac{\mathrm{d}\boldsymbol{v}_i^d}{\mathrm{d}t_0}=\boldsymbol{f}_i^d,\qquad \frac{\mathrm{d}\hat{\boldsymbol{q}}_i^d}{\mathrm{d}t_0}=-\frac{1}{2}\boldsymbol{\omega}_i^d\times\hat{\boldsymbol{q}}_i^d+\frac{1}{2}\bar{q}_i^d\boldsymbol{\omega}_i^d$$

$$\frac{\mathrm{d}\bar{q}_i^d}{\mathrm{d}t_0}=-\frac{1}{2}\boldsymbol{\omega}_i^d\cdot\hat{\boldsymbol{q}}_i^d,\qquad J_i\frac{\mathrm{d}\boldsymbol{\omega}_i^d}{\mathrm{d}t_0}=-\boldsymbol{\omega}_i^d\times\left(J_i\boldsymbol{\omega}_i^d\right)+\boldsymbol{\tau}_i^d \quad (5)$$

This is valid because the desired states for each spacecraft are the same as the actual states for each corresponding place holder, which satisfies the translational and rotational dynamics.

The proposed control force for the ith spacecraft is given by

$$\boldsymbol{f}_i=m_i\left[\dot{\boldsymbol{v}}_i^d-K_{\mathrm{ri}}\left(\boldsymbol{r}_i-\boldsymbol{r}_i^d\right)-K_{\mathrm{vi}}\left(\boldsymbol{v}_i-\boldsymbol{v}_i^d\right)\right] \quad (6)$$

where m_i is the mass of the ith spacecraft and K_{ri} and K_{vi} are symmetric positive definite matrices.

The proposed control torque for the ith spacecraft is given by

$$\boldsymbol{\tau}_i=J_i\dot{\boldsymbol{\omega}}_i^d+\tfrac{1}{2}\boldsymbol{\omega}_i\times J_i\left(\boldsymbol{\omega}_i+\boldsymbol{\omega}_i^d\right)-k_{\mathrm{qi}}\widehat{\boldsymbol{q}_i^{d*}\boldsymbol{q}_i}-K_{\omega i}\left(\boldsymbol{\omega}_i-\boldsymbol{\omega}_i^d\right) \quad (7)$$

where J_i is the moment of inertia of the ith spacecraft, k_{qi} is a positive scalar, $K_{\omega i}$ is a symmetric positive definite matrix, and $\hat{\boldsymbol{q}}$ represents the vector part of the quaternion.

Equations (6) and (7) require both $\boldsymbol{X}_i^d$ and $\dot{\boldsymbol{X}}_i^d$, which are obtained from $\boldsymbol{\xi}_i$ and $\dot{\boldsymbol{\xi}}_i$ using Eqs. (1) and (2).

B. Formation Control Strategies for Each Virtual Structure Instantiation

As in Sec. III.C, $\boldsymbol{\xi}_i$ is the ith coordination vector instantiation and $\boldsymbol{\xi}^{d(k)}$ is the current desired constant goal for the coordination vector instantiations, that is, the current formation pattern. For notation simplicity we hereafter use $\boldsymbol{\xi}^d$ instead of $\boldsymbol{\xi}^{d(k)}$ to represent a certain formation pattern to be achieved. Define

$$\tilde{\boldsymbol{\xi}}_i=\boldsymbol{\xi}_i-\boldsymbol{\xi}^d=\left[\tilde{\boldsymbol{r}}_{\mathrm{Fi}}^T,\tilde{\boldsymbol{v}}_{\mathrm{Fi}}^T,\tilde{\boldsymbol{q}}_{\mathrm{Fi}}^T,\tilde{\boldsymbol{\omega}}_{\mathrm{Fi}}^T,\tilde{\boldsymbol{\lambda}}_{\mathrm{Fi}}^T,\dot{\tilde{\boldsymbol{\lambda}}}_{\mathrm{Fi}}^T\right]^T$$

as the error state for the ith coordination vector instantiation. There are two objectives for the instantiation of the coordination vector implemented in each spacecraft. The first objective is to its desired constant goal $\boldsymbol{\xi}^d$ defined by the formation pattern. The second objective is to synchronize each instantiation, that is, $\boldsymbol{\xi}_1=\boldsymbol{\xi}_2=\cdots=\boldsymbol{\xi}_N$. Following the idea introduced in Refs. 26 and 27, where behavior-based strategies are used to realize goal seeking and formation keeping for each agent, we apply behavior-based strategies to synchronize the coordination vector instantiations during the maneuver as well as evolve it to its desired goal at the end of the maneuver.

Define E_G as the goal seeking error to represent the total error between the current instantiation $\boldsymbol{\xi}_i$ and the desired goal $\boldsymbol{\xi}^d$:

$$E_G(t)=\sum_{i=1}^{N}\left\|\boldsymbol{\xi}_i-\boldsymbol{\xi}^d\right\|^2$$

Also define E_S as the synchronization error to represent the total synchronization error between neighboring instantiations:

$$E_S(t)=\sum_{i=1}^{N}\|\boldsymbol{\xi}_i-\boldsymbol{\xi}_{i+1}\|^2$$

where the summation index i is defined modulo N, that is, $\boldsymbol{\xi}_{N+1}=\boldsymbol{\xi}_1$ and $\boldsymbol{\xi}_0=\boldsymbol{\xi}_N$. Defining $E(t)=E_G(t)+E_S(t)$, then the control objective is to drive $E(t)$ to zero asymptotically.

Because the coordination vector represents the states of the virtual structure, we suppose that the ith coordination vector instantiation satisfies the following rigid-body dynamics:

$$\begin{pmatrix}\dot{\boldsymbol{r}}_{\mathrm{Fi}}\\ m_F\dot{\boldsymbol{v}}_{\mathrm{Fi}}\\ \dot{\boldsymbol{q}}_{\mathrm{Fi}}\\ J_F\dot{\boldsymbol{\omega}}_{\mathrm{Fi}}\\ \dot{\boldsymbol{\lambda}}_{\mathrm{Fi}}\\ \ddot{\boldsymbol{\lambda}}_{\mathrm{Fi}}\end{pmatrix}=\begin{pmatrix}\boldsymbol{v}_{\mathrm{Fi}}\\ \boldsymbol{f}_{\mathrm{Fi}}\\ \tfrac{1}{2}\Omega(\boldsymbol{\omega}_{\mathrm{Fi}})\boldsymbol{q}_{\mathrm{Fi}}\\ -\boldsymbol{\omega}_{\mathrm{Fi}}\times J_F\boldsymbol{\omega}_{\mathrm{Fi}}+\boldsymbol{\tau}_{\mathrm{Fi}}\\ \dot{\boldsymbol{\lambda}}_{\mathrm{Fi}}\\ \boldsymbol{\nu}_{\mathrm{Fi}}\end{pmatrix} \quad (8)$$

where m_F and J_F are the virtual mass and virtual inertia of the virtual structure, $\boldsymbol{f}_{\mathrm{Fi}}$ and $\boldsymbol{\tau}_{\mathrm{Fi}}$ are the virtual force and virtual torque exerted on the ith implementation of the virtual structure, and $\boldsymbol{\nu}_{\mathrm{Fi}}$ is the virtual control effort used to expand or contract the formation.

The tracking performance for the ith spacecraft is defined as $e_{\mathrm{Ti}}=\|\tilde{X}_i\|^2$. Define $\Gamma_{\mathrm{Gi}}=D_G+K_Fe_{\mathrm{Ti}}$ to incorporate formation feedback from the ith spacecraft to the ith coordination vector implementation, where D_G and K_F are symmetric positive definite matrices. Obviously, Γ_{Gi} is also a positive definite matrix. If we let $K_F=0$, there is no formation feedback. The proposed control force $\boldsymbol{f}_{\mathrm{Fi}}$ is given by

$$\begin{aligned}\boldsymbol{f}_{\mathrm{Fi}}=m_F\Big\{&-K_G\left(\boldsymbol{r}_{\mathrm{Fi}}-\boldsymbol{r}_F^d\right)-\Gamma_{\mathrm{Gi}}\boldsymbol{v}_{\mathrm{Fi}}-K_S\left[\boldsymbol{r}_{\mathrm{Fi}}-\boldsymbol{r}_{F(i+1)}\right]\\ &-D_S\left[\boldsymbol{v}_{\mathrm{Fi}}-\boldsymbol{v}_{F(i+1)}\right]-K_S\left[\boldsymbol{r}_{\mathrm{Fi}}-\boldsymbol{r}_{F(i-1)}\right]\\ &-D_S\left[\boldsymbol{v}_{\mathrm{Fi}}-\boldsymbol{v}_{F(i-1)}\right]\Big\}\end{aligned} \quad (9)$$

where K_G is a symmetric positive definite matrix and K_S and D_S are symmetric positive semidefinite matrices.

The proposed control torque $\boldsymbol{\tau}_{\mathrm{Fi}}$ is given by

$$\begin{aligned}\boldsymbol{\tau}_{\mathrm{Fi}}=&-k_G\widehat{\boldsymbol{q}_F^{d*}\boldsymbol{q}_{\mathrm{Fi}}}-\Gamma_{\mathrm{Gi}}\boldsymbol{\omega}_{\mathrm{Fi}}-k_S\widehat{\boldsymbol{q}_{F(i+1)}^{*}\boldsymbol{q}_{\mathrm{Fi}}}-D_S\left[\boldsymbol{\omega}_{\mathrm{Fi}}-\boldsymbol{\omega}_{F(i+1)}\right]\\ &-k_S\widehat{\boldsymbol{q}_{F(i-1)}^{*}\boldsymbol{q}_{\mathrm{Fi}}}-D_S\left[\boldsymbol{\omega}_{\mathrm{Fi}}-\boldsymbol{\omega}_{F(i-1)}\right]\end{aligned} \quad (10)$$

where $k_G>0$ and $k_S\geq 0$ are scalars, Γ_{Gi} follows the same definition as just stated, D_S is a symmetric positive semidefinite matrix, and $\hat{\boldsymbol{q}}$ represents the vector part of the quaternion.

Similar to Eq. (9), the proposed control effort $\boldsymbol{\nu}_{\mathrm{Fi}}$ is given by

$$\boldsymbol{\nu}_{\mathrm{Fi}} = -K_G\left(\boldsymbol{\lambda}_{\mathrm{Fi}} - \boldsymbol{\lambda}_F^d\right) - \Gamma_{\mathrm{Gi}}\dot{\boldsymbol{\lambda}}_{\mathrm{Fi}} - K_S\left[\boldsymbol{\lambda}_{\mathrm{Fi}} - \boldsymbol{\lambda}_{F(i+1)}\right] - D_S\left[\dot{\boldsymbol{\lambda}}_{\mathrm{Fi}} - \dot{\boldsymbol{\lambda}}_{F(i+1)}\right] - K_S\left[\boldsymbol{\lambda}_{\mathrm{Fi}} - \boldsymbol{\lambda}_{F(i-1)}\right] - D_S\left[\dot{\boldsymbol{\lambda}}_{\mathrm{Fi}} - \dot{\boldsymbol{\lambda}}_{F(i-1)}\right] \tag{11}$$

where K_G is a symmetric positive definite matrix, Γ_{Gi} follows the same definition as just stated, and K_S and D_S are symmetric positive semidefinite matrices.

Note that the matrices in Eqs. (9–11) can be chosen differently based on specific requirements. In Eqs. (9–11), the first two terms are used to drive $E_G \to 0$, the third and fourth terms are used to synchronize the ith and $(i+1)$th coordination vector instantiations, and the fifth and sixth terms are used to synchronize the ith and $(i-1)$th coordination vector instantiations. The second term, that is, the formation feedback term, is also used to slow down the ith virtual structure implementation when the ith spacecraft has a large tracking error. This strategy needs each spacecraft to know its neighboring coordination vector instantiations, which can be accomplished by nearest neighbor communication. From Eqs. (9–11), we can also see that besides $\boldsymbol{\xi}_{i-1}$, $\boldsymbol{\xi}_i$, and $\boldsymbol{\xi}_{i+1}$ the control laws for the ith coordination vector instantiation also require the current constant formation pattern $\boldsymbol{\xi}^d$ and $\tilde{\boldsymbol{X}}_i$ through the formation feedback gain matrix Γ_{Gi}.

C. Convergence Analysis

The following lemmas will be used to prove our main result.

Lemma 1: If both the unit quaternion and angular velocity pairs $(\boldsymbol{q}_s, \boldsymbol{\omega}_s)$ and $(\boldsymbol{q}_p, \boldsymbol{\omega}_p)$ satisfy the rotational dynamics (4) with moment of inertia J and with control torque $\boldsymbol{\tau}_s$ and $\boldsymbol{\tau}_p$, respectively, $\delta\boldsymbol{\omega} = \boldsymbol{\omega}_s - \boldsymbol{\omega}_p$ and $\delta\boldsymbol{q} = \boldsymbol{q}_s - \boldsymbol{q}_p$ with $\delta\hat{\boldsymbol{q}} = \hat{\boldsymbol{q}}_s - \hat{\boldsymbol{q}}_p$ and $\delta\bar{q} = \bar{q}_s - \bar{q}_p$, and $V_1 = \delta\bar{q}^2 + \delta\hat{\boldsymbol{q}}\cdot\delta\hat{\boldsymbol{q}}$ and $V_2 = \frac{1}{2}\delta\boldsymbol{\omega}\cdot J\delta\boldsymbol{\omega}$, then $\dot{V}_1 = \delta\boldsymbol{\omega}\cdot\widehat{\boldsymbol{q}_p^*\boldsymbol{q}_s}$ and $\dot{V}_2 = \delta\boldsymbol{\omega}\cdot[\boldsymbol{\tau}_s - \boldsymbol{\tau}_p - \frac{1}{2}(\boldsymbol{\omega}_s \times J\delta\boldsymbol{\omega})]$.

Proof: Identical to the proof for attitude control in Ref. 16 by replacing $\boldsymbol{q}_i$ with $\boldsymbol{q}_p$, $\boldsymbol{\omega}_i$ with $\boldsymbol{\omega}_p$, $\boldsymbol{q}_i^d$ with $\boldsymbol{q}_s$, and $\boldsymbol{\omega}_i^d$ with $\boldsymbol{\omega}_s$. ∎

For a vector $\boldsymbol{x}$ we use $\boldsymbol{x}^T\boldsymbol{x}$ or $\|\boldsymbol{x}\|^2$ to represent the vector dot product $\boldsymbol{x}\cdot\boldsymbol{x}$ hereafter.

Lemma 2: If $A \in \mathbb{R}^{k\times k}$ and $B \in \mathbb{R}^{l\times l}$ are symmetric positive semidefinite matrices, then $A \otimes B$ is positive semidefinite, where $\otimes$ denotes the Kronecker product. Moreover, if both A and B are symmetric positive definite, then so is $A \otimes B$.

Proof: See Ref. 31. ∎

Lemma 3: If C is a circulant matrix with the first row given by $[2, -1, 0, \ldots, 0, -1] \in \mathbb{R}^N$, then $C \in \mathbb{R}^{N\times N}$ is symmetric positive semidefinite. Let $P \in \mathbb{R}^{p\times p}$ and $\boldsymbol{Z} = [z_1^T, \ldots, z_N^T]^T$, where $z_i \in \mathbb{R}^p$. If the terms $P(z_i - z_{i-1}) + P(z_i - z_{i+1})$ are stacked in a column vector, the resulting vector can be written as $(C \otimes P)\boldsymbol{Z}$.

Proof: See Ref. 26. ∎

From Eqs. (3), (4), (6), and (7), the dynamics for the ith spacecraft can be represented by $\dot{\tilde{\boldsymbol{X}}}_i = f(\tilde{\boldsymbol{X}}_i, \boldsymbol{\xi}_i)$, where $f(\cdot,\cdot)$ can be determined from those equations. From Eqs. (8–11), the dynamics for the ith coordination vector instantiation can be represented by $\dot{\boldsymbol{\xi}}_i = g(\boldsymbol{\xi}_{i-1}, \boldsymbol{\xi}_i, \boldsymbol{\xi}_{i+1}, \tilde{\boldsymbol{X}}_i)$, where $g(\cdot,\cdot,\cdot,\cdot)$ can also be determined from those equations. Therefore, the coupled dynamics of the whole system composed of N spacecraft and N coordination vector instantiations are time invariant with states $\tilde{\boldsymbol{X}}_i$ and $\boldsymbol{\xi}_i$, $i = 1, \ldots, N$. LaSalle's invariance principle will be used to prove the main theorem for convergence of the whole system.

Theorem 1: If the control laws for each spacecraft are given by Eqs. (6) and (7) and the control laws for each coordination vector instantiation are given by Eqs. (9–11), then

$$\sum_{i=1}^N e_{\mathrm{Ti}} + E(t) \to 0$$

asymptotically.

Proof:

For the whole system consisting of N spacecraft and N coordination vector instantiations, consider the Lyapunov function candidate:

$$V = V_{\mathrm{sp}} + V_{\mathrm{Ft}} + V_{\mathrm{Fr}} + V_{\mathrm{Fe}} \tag{12}$$

where

$$V_{\mathrm{sp}} = \sum_{i=1}^N \left(\frac{1}{2}\tilde{\boldsymbol{r}}_i^T K_{\mathrm{ri}}\tilde{\boldsymbol{r}}_i + \frac{1}{2}\tilde{\boldsymbol{v}}_i^T\tilde{\boldsymbol{v}}_i + k_{\mathrm{qi}}\tilde{\boldsymbol{q}}_i^T\tilde{\boldsymbol{q}}_i + \frac{1}{2}\tilde{\boldsymbol{\omega}}_i^T J_i\tilde{\boldsymbol{\omega}}_i\right)$$

$$V_{\mathrm{Ft}} = \frac{1}{2}\sum_{i=1}^N \left[\boldsymbol{r}_{\mathrm{Fi}} - \boldsymbol{r}_{F(i+1)}\right]^T K_S\left[\boldsymbol{r}_{\mathrm{Fi}} - \boldsymbol{r}_{F(i+1)}\right] + \frac{1}{2}\sum_{i=1}^N\left(\tilde{\boldsymbol{r}}_{\mathrm{Fi}}^T K_G\tilde{\boldsymbol{r}}_{\mathrm{Fi}} + \boldsymbol{v}_{\mathrm{Fi}}^T\boldsymbol{v}_{\mathrm{Fi}}\right)$$

$$V_{\mathrm{Fr}} = \sum_{i=1}^N k_S\left[\boldsymbol{q}_{\mathrm{Fi}} - \boldsymbol{q}_{F(i+1)}\right]^T\left[\boldsymbol{q}_{\mathrm{Fi}} - \boldsymbol{q}_{F(i+1)}\right] + \sum_{i=1}^N\left(k_G\tilde{\boldsymbol{q}}_{\mathrm{Fi}}^T\tilde{\boldsymbol{q}}_{\mathrm{Fi}} + \frac{1}{2}\boldsymbol{\omega}_{\mathrm{Fi}}^T J_F\boldsymbol{\omega}_{\mathrm{Fi}}\right)$$

$$V_{\mathrm{Fe}} = \frac{1}{2}\sum_{i=1}^N\left[\boldsymbol{\lambda}_{\mathrm{Fi}} - \boldsymbol{\lambda}_{F(i+1)}\right]^T K_S\left[\boldsymbol{\lambda}_{\mathrm{Fi}} - \boldsymbol{\lambda}_{F(i+1)}\right] + \frac{1}{2}\sum_{i=1}^N\left(\tilde{\boldsymbol{\lambda}}_{\mathrm{Fi}}^T K_G\tilde{\boldsymbol{\lambda}}_{\mathrm{Fi}} + \dot{\boldsymbol{\lambda}}_{\mathrm{Fi}}^T\dot{\boldsymbol{\lambda}}_{\mathrm{Fi}}\right)$$

With the proposed control force (6) for each spacecraft, the second equation in the translational dynamics (3) for the ith spacecraft can be rewritten as $\dot{\tilde{\boldsymbol{v}}}_i = -K_{\mathrm{ri}}\tilde{\boldsymbol{r}}_i - K_{\mathrm{vi}}\tilde{\boldsymbol{v}}_i$. Applying Lemma 1, the derivative of V_{sp} is

$$\dot{V}_{\mathrm{sp}} = \sum_{i=1}^N\left(-\tilde{\boldsymbol{v}}_i^T K_{\mathrm{vi}}\tilde{\boldsymbol{v}}_i\right) + \sum_{i=1}^N\tilde{\boldsymbol{\omega}}_i^T \cdot\left[k_{\mathrm{qi}}\widehat{\boldsymbol{q}_i^{d*}\boldsymbol{q}_i} + \boldsymbol{\tau}_i - \boldsymbol{\tau}_i^d - \frac{1}{2}(\boldsymbol{\omega}_i \times J_i\tilde{\boldsymbol{\omega}}_i)\right]$$

From Eq. (5) $\boldsymbol{\tau}_i^d = J_i\dot{\boldsymbol{\omega}}_i^d + \boldsymbol{\omega}_i^d \times (J_i\boldsymbol{\omega}_i^d)$. With the proposed control torque (7) for each spacecraft, after some manipulation we know that

$$\dot{V}_{\mathrm{sp}} = \sum_{i=1}^N\left(-\tilde{\boldsymbol{v}}_i^T K_{\mathrm{vi}}\tilde{\boldsymbol{v}}_i - \tilde{\boldsymbol{\omega}}_i^T K_{\omega i}\tilde{\boldsymbol{\omega}}_i\right) \le 0 \tag{13}$$

Differentiating V_{Ft}, we can get

$$\dot{V}_{\mathrm{Ft}} = \sum_{i=1}^N v_{\mathrm{Fi}}^T\left\{K_S\left[\boldsymbol{r}_{\mathrm{Fi}} - \boldsymbol{r}_{F(i+1)}\right] + K_S\left[\boldsymbol{r}_{\mathrm{Fi}} - \boldsymbol{r}_{F(i-1)}\right] + K_G\tilde{\boldsymbol{r}}_{\mathrm{Fi}} + \frac{\boldsymbol{f}_{\mathrm{Fi}}}{m_F}\right\}$$

With the proposed control force (9) for each coordination vector instantiation,

$$\dot{V}_{\mathrm{Ft}} = -\sum_{i=1}^N\left\{\boldsymbol{v}_{\mathrm{Fi}}^T\Gamma_{\mathrm{Gi}}\boldsymbol{v}_{\mathrm{Fi}} + \left[\boldsymbol{v}_{\mathrm{Fi}} - \boldsymbol{v}_{F(i+1)}\right]^T D_S\left[\boldsymbol{v}_{\mathrm{Fi}} - \boldsymbol{v}_{F(i+1)}\right]\right\} \le 0 \tag{14}$$

Applying Lemma 1, the derivative of V_{Fr} is

$$\dot{V}_{\mathrm{Fr}} = \sum_{i=1}^N\left[\boldsymbol{\omega}_{\mathrm{Fi}} - \boldsymbol{\omega}_{F(i+1)}\right]^T k_S\widehat{\boldsymbol{q}_{F(i+1)}^*\boldsymbol{q}_{\mathrm{Fi}}} + \sum_{i=1}^N\boldsymbol{\omega}_{\mathrm{Fi}}^T\left(k_G\widehat{\boldsymbol{q}_F^{d*}\boldsymbol{q}_{\mathrm{Fi}}} + \boldsymbol{\tau}_{\mathrm{Fi}} - \frac{1}{2}\boldsymbol{\omega}_{\mathrm{Fi}} \times J_F\boldsymbol{\omega}_{\mathrm{Fi}}\right)$$

After some manipulation

$$\dot V_{\rm Fr} = \sum_{i=1}^{N} \omega_{\rm Fi}^T\Big[k_S\widehat{\boldsymbol q^*_{F(i+1)}\boldsymbol q_{\rm Fi}} - k_S\widehat{\boldsymbol q^*_{\rm Fi}\boldsymbol q_{F(i-1)}} + k_G\widehat{\boldsymbol q_F^{d*}\boldsymbol q_{\rm Fi}} + \boldsymbol\tau_{\rm Fi}\Big]$$

With the proposed control torque (10) for each coordination vector instantiation,

$$\dot V_{\rm Fr} = -\sum_{i=1}^{N}\Big\{\boldsymbol\omega_{\rm Fi}^T\Gamma_{\rm Gi}\boldsymbol\omega_{\rm Fi} + \big[\boldsymbol\omega_{\rm Fi} - \boldsymbol\omega_{F(i+1)}\big]^T \cdot D_S\big[\boldsymbol\omega_{\rm Fi} - \boldsymbol\omega_{F(i+1)}\big]\Big\} \le 0 \tag{15}$$

Similar to $\dot V_{\rm Ft}$, with the proposed control effort (11) for each coordination vector instantiation, the derivative of $V_{\rm Fe}$ is

$$\dot V_{\rm Fe} = -\sum_{i=1}^{N}\Big\{\dot{\boldsymbol\lambda}_{\rm Fi}^T\Gamma_{\rm Gi}\dot{\boldsymbol\lambda}_{\rm Fi} + \big[\dot{\boldsymbol\lambda}_{\rm Fi} - \dot{\boldsymbol\lambda}_{F(i+1)}\big]^T \cdot D_S\big[\dot{\boldsymbol\lambda}_{\rm Fi} - \dot{\boldsymbol\lambda}_{F(i+1)}\big]\Big\} \le 0 \tag{16}$$

From Eqs. (13–16), it is obvious that $\dot V = \dot V_{\rm sp} + \dot V_{\rm Ft} + \dot V_{\rm Fr} + \dot V_{\rm Fe} \le 0$. Let $\Sigma = \{(\tilde{\boldsymbol X}_1,\dots,\tilde{\boldsymbol X}_N,\tilde{\boldsymbol\xi}_1,\dots,\tilde{\boldsymbol\xi}_N)|\dot V = 0\}$, and let $\bar\Sigma$ be the largest invariant set in Σ. On $\bar\Sigma$, $\dot V \equiv 0$, that is, $\dot V_{\rm sp} = \dot V_{\rm Ft} = \dot V_{\rm Fr} = \dot V_{\rm Fe} \equiv 0$, which implies that $\tilde{\boldsymbol v}_i \equiv 0, \tilde{\boldsymbol\omega}_i \equiv 0, \boldsymbol v_{\rm Fi} \equiv 0, \boldsymbol\omega_{\rm Fi} \equiv 0, \dot{\boldsymbol\lambda}_{\rm Fi} \equiv 0, i = 1,\dots,N$.

Because $\tilde{\boldsymbol v}_i \equiv 0$, we know that $\tilde{\boldsymbol r}_i = 0$ from Eqs. (3) and (6). Because $\tilde{\boldsymbol\omega}_i \equiv 0$, we also know that $\widehat{\boldsymbol q_i^{d*}\boldsymbol q_i} = 0$ from Eqs. (4) and (7), which then implies that $\boldsymbol q_i = \boldsymbol q_i^d$, that is, $\tilde{\boldsymbol q}_i = 0$.

Then following $\boldsymbol v_{\rm Fi} \equiv 0$, from Eq. (9) and the second equation in Eq. (8), it can be seen that

$$K_G\tilde{\boldsymbol r}_{\rm Fi} + K_S\big[\boldsymbol r_{\rm Fi} - \boldsymbol r_{F(i+1)}\big] + K_S\big[\boldsymbol r_{\rm Fi} - \boldsymbol r_{F(i-1)}\big] = 0 \qquad i = 1,\dots,N$$

which is equivalent to

$$K_G\tilde{\boldsymbol r}_{\rm Fi} + K_S\big[\tilde{\boldsymbol r}_{\rm Fi} - \tilde{\boldsymbol r}_{F(i+1)}\big] + K_S\big[\tilde{\boldsymbol r}_{\rm Fi} - \tilde{\boldsymbol r}_{F(i-1)}\big] = 0 \qquad i = 1,\dots,N \tag{17}$$

From lemma 3, Eq. (17) can also be written as $(I_N \otimes K_G + C \otimes K_S)\tilde{\boldsymbol r}_F = 0$, where $\tilde{\boldsymbol r}_F = [\tilde{\boldsymbol r}_{F1}^T,\dots,\tilde{\boldsymbol r}_{\rm FN}^T]^T$, I_N is an $N\times N$ identity matrix, and C is the circulant matrix defined in lemma 3. Based on lemmas 2 and 3, $I_N \otimes K_G$ is positive definite and $C \otimes K_S$ is positive semidefinite. Thus we know that $\tilde{\boldsymbol r}_F = 0$.

Following a similar procedure as just stated, we can also show that $\tilde{\boldsymbol\lambda}_{\rm Fi} = 0$ because $\dot{\boldsymbol\lambda}_{\rm Fi} \equiv 0$.

Also following $\boldsymbol\omega_{\rm Fi} \equiv 0$, from Eq. (10) and the fourth equation in Eq. (8), we know that

$$k_G\widehat{\boldsymbol q_F^{d*}\boldsymbol q_{\rm Fi}} + k_S\widehat{\boldsymbol q^*_{F(i+1)}\boldsymbol q_{\rm Fi}} + k_S\widehat{\boldsymbol q^*_{F(i-1)}\boldsymbol q_{\rm Fi}} = 0, \qquad i = 1,\dots,N \tag{18}$$

Because the quaternion multiplication is associative, we know that

$$\boldsymbol q^*_{F(i+1)}\boldsymbol q_{\rm Fi} = \boldsymbol q^*_{F(i+1)}\mathbf 1\boldsymbol q_{\rm Fi} = \boldsymbol q^*_{F(i+1)}\big(\boldsymbol q_F^d\boldsymbol q_F^{d*}\big)\boldsymbol q_{\rm Fi} = \big[\boldsymbol q^*_{F(i+1)}\boldsymbol q_F^d\big]\big(\boldsymbol q_F^{d*}\boldsymbol q_{\rm Fi}\big)$$

where $\mathbf 1$ is the multiplicative identity quaternion defined in Sec. II.B. Therefore, Eq. (18) is equivalent to

$$k_G\widehat{\boldsymbol q_F^{d*}\boldsymbol q_{\rm Fi}} + k_S\widehat{\big[\boldsymbol q^*_{F(i+1)}\boldsymbol q_F^d\big]\big(\boldsymbol q_F^{d*}\boldsymbol q_{\rm Fi}\big)} + k_S\widehat{\big[\boldsymbol q^*_{F(i-1)}\boldsymbol q_F^d\big]\big(\boldsymbol q_F^{d*}\boldsymbol q_{\rm Fi}\big)} = 0 \qquad i = 1,\dots,N \tag{19}$$

Following Ref. 27 and applying the property of the unit quaternion, Eq. (19) can be written as $\boldsymbol p_i^*\widehat{(\boldsymbol q_F^{d*}\boldsymbol q_{\rm Fi})} = 0$, where $\boldsymbol p_i = k_G\mathbf 1 + k_S[\boldsymbol q_F^{d*}\boldsymbol q_{F(i+1)}] + k_S[\boldsymbol q_F^{d*}\boldsymbol q_{F(i-1)}]$.

Compared with Eq. (7) in Ref. 27, Eq. (19) has the same form when we treat $\boldsymbol q_i$ as $\boldsymbol q_F^{d*}\boldsymbol q_{\rm Fi}$ and k_F as k_S and delete $k_e\widehat{\boldsymbol q}_{\rm iR}$ term in Eq. (7) in Ref. 27. It can be verified that their proof for $\widehat{\boldsymbol q_i} = 0$ is still valid when $k_e\widehat{\boldsymbol q}_{\rm iR}$ term is omitted, which is only used to guarantee the rotation of the spacecraft about a defined axis.

Then following the result $\widehat{\boldsymbol q_i} = 0$ in Ref. 27, we can show that $\widehat{\boldsymbol q_F^{d*}\boldsymbol q_{\rm Fi}} = 0$, which implies that $\boldsymbol q_{\rm Fi} = \boldsymbol q_F^d$, that is, $\tilde{\boldsymbol q}_{\rm Fi} = 0$.

Therefore, by LaSalle's invariance principle $\|\tilde{\boldsymbol X}_i\| \to 0$, $\|\tilde{\boldsymbol\xi}_i\| \to 0$, and $\|\boldsymbol\xi_i - \boldsymbol\xi_{i+1}\| \to 0$, $i = 1,\dots,N$. Accordingly,

$$\sum_{i=1}^{N} e_{\rm Ti} + E(t) \to 0$$

asymptotically. ■

From theorem 1 we can see that each virtual structure instantiation will achieve its final goal asymptotically, and each spacecraft will also track its desired state specified by the virtual structure asymptotically during the maneuver. Therefore, the formation maneuver can be achieved asymptotically.

Because PD-like control laws are used for each spacecraft and each coordination vector instantiation, the transient specifications for each spacecraft and each coordination vector instantiation can be satisfied by designing corresponding gain matrices in the control laws following the design procedure for the coefficients of a second-order system. Moreover, for each spacecraft, if we define a translational tracking error for the ith spacecraft as $E_{\rm ti} = \frac{1}{2}\tilde{\boldsymbol r}_i^T K_{\rm ri}\tilde{\boldsymbol r}_i + \frac{1}{2}\|\tilde{\boldsymbol v}_i\|^2$, $E_{\rm ti}$ decreases during the maneuver and $\tilde{\boldsymbol r}_i^T K_{\rm ri}\tilde{\boldsymbol r}_i$ is bounded by $2E_{\rm ti}(0) - \|\tilde{\boldsymbol v}_i\|^2$ following the proof for $\dot V_{\rm sp}$. Similarly, if we define a rotational tracking error as $E_{\rm ri} = k_{\rm qi}\|\tilde{\boldsymbol q}_i\|^2 + \frac{1}{2}\tilde{\boldsymbol\omega}_i J_i\tilde{\boldsymbol\omega}_i$, $E_{\rm ri}$ decreases during the maneuver, and $\|\tilde{\boldsymbol q}_i\|^2$ is bounded by $(1/k_{\rm qi})[E_{\rm ri}(0) - \frac{1}{2}\tilde{\boldsymbol\omega}_i J_i\tilde{\boldsymbol\omega}_i]$. For each coordination vector instantiation, following the proof for $\dot V_{\rm Ft}$, $\dot V_{\rm Fr}$, and $\dot V_{\rm Fe}$, we know that $V_{\rm Ft}$, $V_{\rm Fr}$, and $V_{\rm Fe}$ are bounded by $V_{\rm Ft}(0)$, $V_{\rm Fr}(0)$, and $V_{\rm Fe}(0)$, respectively. Therefore,

$$\sum_{i=1}^{N}\big[\boldsymbol r_{\rm Fi} - \boldsymbol r_{F(i+1)}\big]^T K_S\big[\boldsymbol r_{\rm Fi} - \boldsymbol r_{F(i+1)}\big] \le 2V_{\rm Ft}(0)$$

$$\sum_{i=1}^{N}\tilde{\boldsymbol r}_{\rm Fi}^T K_G\tilde{\boldsymbol r}_{\rm Fi} \le 2V_{\rm Ft}(0), \qquad \sum_{i=1}^{N}\|\boldsymbol q_{\rm Fi} - \boldsymbol q_{F(i+1)}\|^2 \le \frac{1}{k_S}V_{\rm Fr}(0)$$

$$\sum_{i=1}^{N}\|\tilde{\boldsymbol q}_{\rm Fi}\|^2 \le \frac{1}{k_G}V_{\rm Fr}(0)$$

$$\sum_{i=1}^{N}\big[\boldsymbol\lambda_{\rm Fi} - \boldsymbol\lambda_{F(i+1)}\big]^T K_S\big[\boldsymbol\lambda_{\rm Fi} - \boldsymbol\lambda_{F(i+1)}\big] \le 2V_{\rm Fe}(0)$$

$$\sum_{i=1}^{N}\tilde{\boldsymbol\lambda}_{\rm Fi}^T K_G\tilde{\boldsymbol\lambda}_{\rm Fi} \le 2V_{\rm Fe}(0)$$

V. Simulation Results

In this section we consider a scenario with nine spacecraft. In the scenario a mothership spacecraft with mass equal to 1500 kg is located 1 km away from a plane where eight daughter spacecraft each with mass 150 kg are distributed equally along a circle with a diameter 1 km in the plane. The configuration of the nine spacecraft is shown in Fig. 3. We assume that the nine spacecraft evolves like a rigid structure, that is, the formation shape is preserved and each spacecraft preserves a fixed relative orientation within the formation throughout the formation maneuvers.

We simulate a scenario when the nine spacecraft start from rest with some initial position and attitude errors and then perform a group rotation of 45 deg about the inertial z axis. Here we assume that each place holder in the formation has the same orientation, that is, $\boldsymbol q_{\rm iF}^d$ is the same for each spacecraft. In simulation, we instantiate a local copy of the coordination vector $\boldsymbol\xi$ in each spacecraft and synchronize them using the control strategy introduced in Sec. IV.B. To show the robustness of the control strategy, we start the coordination vector implementation in each spacecraft at a different time instance

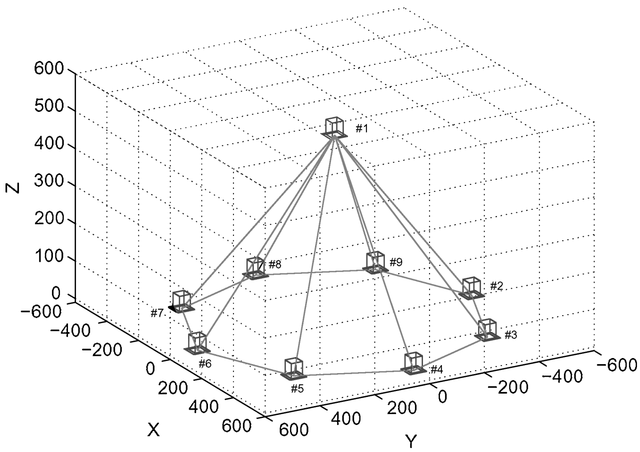

Fig. 3 Geometric configuration of nine spacecraft.

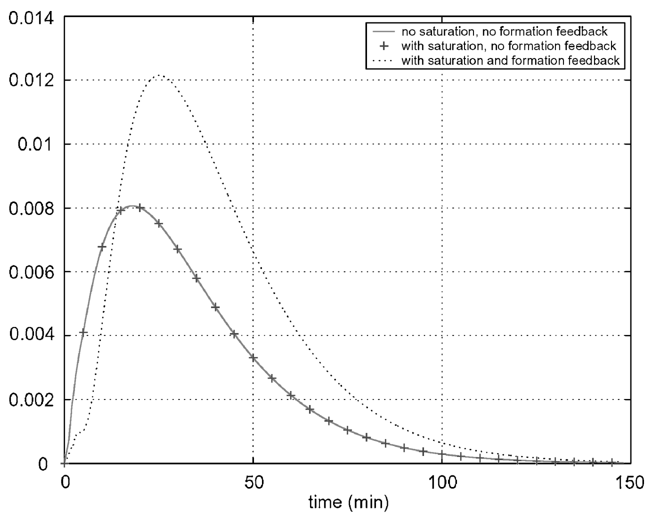

Fig. 4 Average coordination error of the coordination vector instantiations.

and introduce a different sample time varying from 0.4 to 0.6 s for each coordination vector instantiation. Various communication delays are also added among spacecraft. Three cases will be compared in this section. These include cases without actuator saturation and formation feedback (case 1), with actuator saturation but without formation feedback (case 2), with both actuator saturation and formation feedback (case 3). In fact, there is another case without actuator saturation but with formation feedback (case 4). Because there is little difference between this case and case 1, we will not include this case in this section. Here we assume that the control force and control torque for spacecraft 1 are saturated at $|f_x|, |f_y|, |f_z| = 2$ N and $|\tau_x|, |\tau_y|, |\tau_z| = 0.0006$ Nm, respectively, and the control force and control torque for all of the other spacecraft are saturated at $|f_x|, |f_y|, |f_z| = 1$ N and $|\tau_x|, |\tau_y|, |\tau_z| = 0.0003$ Nm, respectively.

In this section the average coordination error is defined as

$$\frac{1}{N}\sum_{i=1}^{N}\|\boldsymbol{\xi}_i - \bar{\boldsymbol{\xi}}\|$$

where

$$\bar{\boldsymbol{\xi}} = \frac{1}{N}\sum_{i=1}^{N}\boldsymbol{\xi}_i$$

The average coordination error in these three cases is plotted in Fig. 4. We can see that each instantiation of the coordination vector is synchronized asymptotically in all cases. Also, the average coordination error is large during the initial time interval because each local instantiation starts at a different time instance. Cases 1 and 2 are identical because the actuator saturation for each spacecraft does not affect the dynamics of the virtual structure when there is no formation feedback from each spacecraft to its coordination vector instantiation. The maximum average coordination error in case 3 is larger than that in the other two cases because formation feedback is introduced for each coordination vector instantiation, which can add some dissimilarities between different instantiations.

In Fig. 5 we plot the absolute position and attitude tracking errors for spacecraft 1, 4, and 7 in these three cases. The position tracking error is defined as $\|\boldsymbol{r}_i - \boldsymbol{r}_i^d\|$, and the attitude tracking error is defined as $\|\boldsymbol{q}_i - \boldsymbol{q}_i^d\|$. We can see the tracking errors in each case

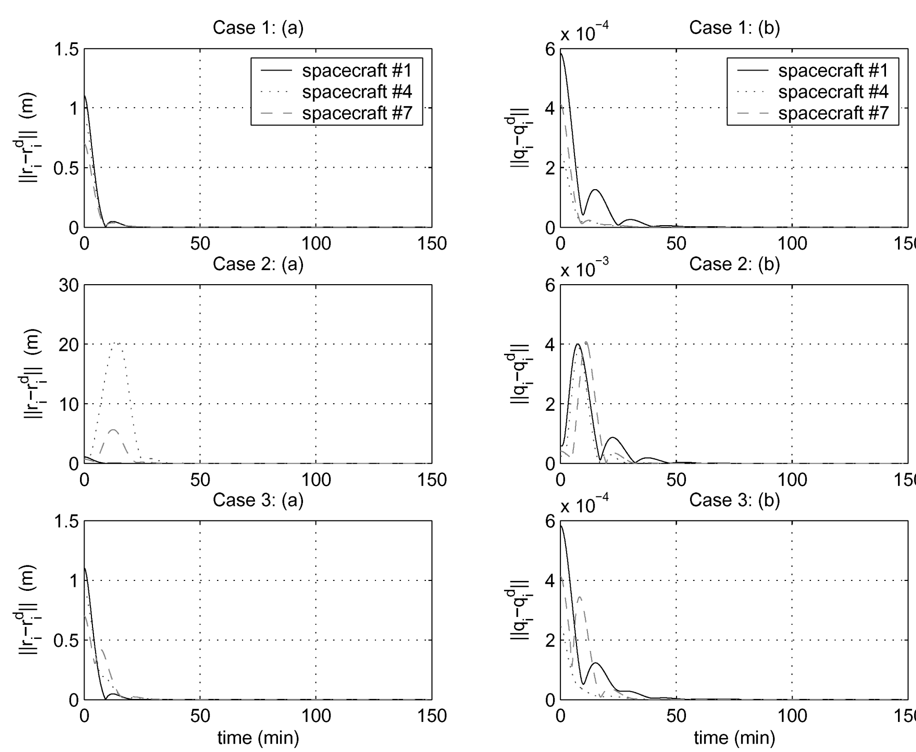

Fig. 5 Absolute position and attitude tracking errors.

will decrease to zero asymptotically by using the control law given in Sec. IV.A. The absolute position and attitude tracking errors in case 2 are much larger than those in the other two cases because of the actuator saturation. In case 3, with formation feedback, the absolute position and attitude tracking errors are similar to those in case 1 even if there is actuator saturation. When we increase the entries in the gain matrix K_F to increase formation feedback, the absolute tracking errors can be decreased further, but the system convergence time will become correspondingly longer.

In Fig. 6 we plot the relative position and attitude errors between some spacecraft in these three cases. Based on the configuration, the desired relative distance between spacecraft 1 and 2 and the desired relative distance between spacecraft 1 and 6 should be equal. The desired relative distance between spacecraft 3 and 7 and the desired relative distance between spacecraft 5 and 9 should also be equal. We plot $|\|\boldsymbol{r}_1 - \boldsymbol{r}_2\| - \|\boldsymbol{r}_1 - \boldsymbol{r}_6\||$ and $|\|\boldsymbol{r}_3 - \boldsymbol{r}_7\| - \|\boldsymbol{r}_5 - \boldsymbol{r}_9\||$ in subplot a. as examples to see how well the formation shape is preserved. The desired relative attitude between each spacecraft should be equal based on our preceding assumption. We plot $\|\boldsymbol{q}_1 - \boldsymbol{q}_4\|$, $\|\boldsymbol{q}_4 - \boldsymbol{q}_7\|$, and $\|\boldsymbol{q}_7 - \boldsymbol{q}_1\|$ in subplot b as examples to see how well the relative orientation relationships between these spacecraft are preserved. Similarly, the relative position tracking errors in case 2 are larger than those in the other two cases because of the control force saturation. In case 3, with formation feedback, the relative position errors are smaller than those in case 2. The relative attitude errors in case 3 are even smaller than those in the other two cases because of the formation feedback.

In Fig. 7 we plot the control effort for spacecraft 1 in these three cases. We can see that both the control force and control torque approach zero asymptotically. We can also see that τ_z saturates in

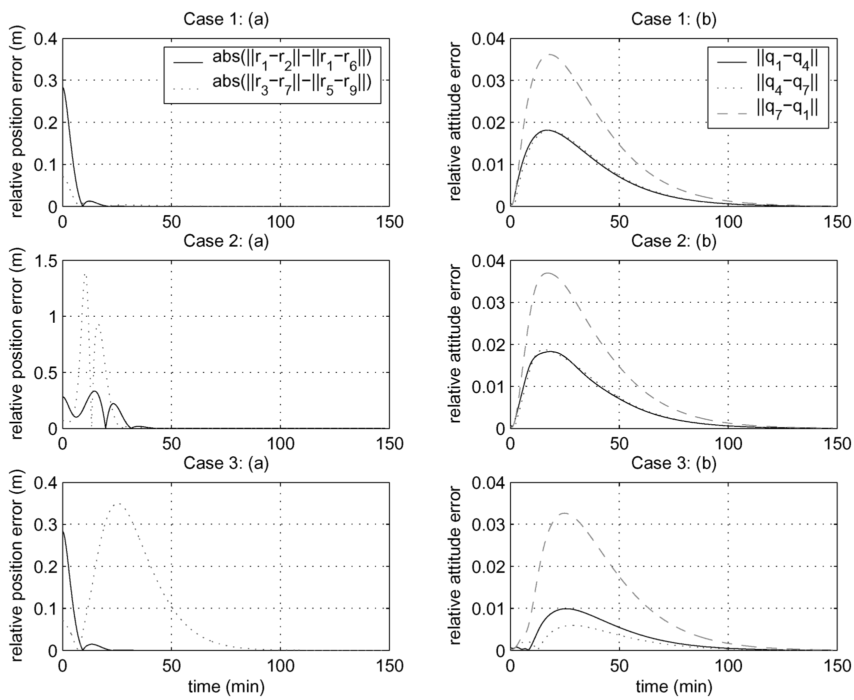

Fig. 6 Relative position and attitude errors.

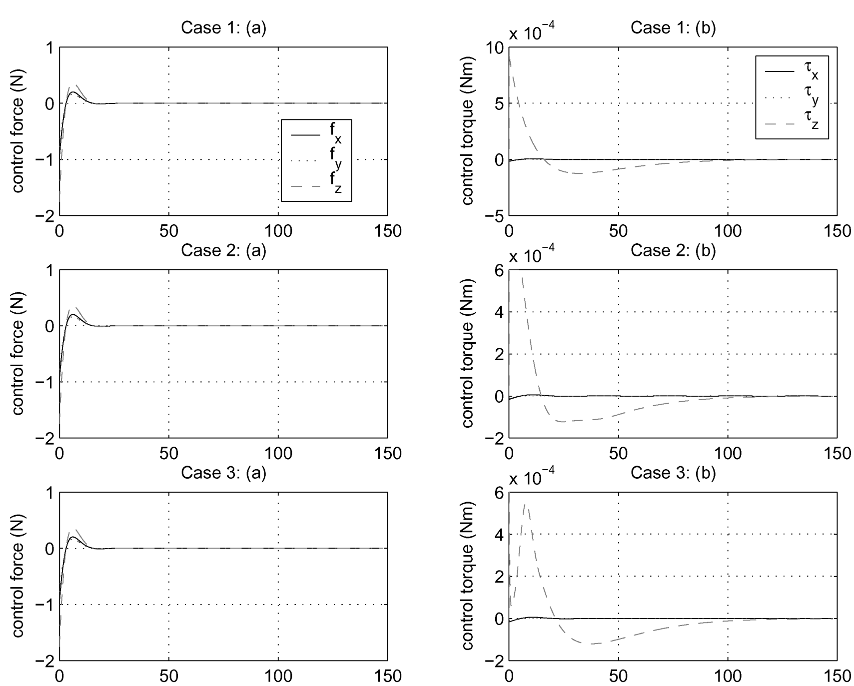

Fig. 7 Control effort for spacecraft 1.

case 2 during the initial time period while this saturation is mitigated with formation feedback introduced in case 3.

VI. Conclusions

In this paper we proposed a decentralized scheme for spacecraft formation control using the virtual structure approach. Through low-bandwidth communication between neighboring spacecraft, the instantiation of the coordination vector in each spacecraft can be synchronized and then used to define the desired states for each spacecraft. Decentralized formation control strategies were presented for each spacecraft to synchronize the coordination vector instantiation and track its desired states. The effectiveness of the proposed strategies was demonstrated through a simulation example.

References

[1]Wang, P. K. C., "Navigation Strategies for Multiple Autonomous Mobile Robots Moving in Formation," *Journal of Robotic Systems*, Vol. 8, No. 2, 1991, pp. 177–195.

[2]Balch, T., and Arkin, R. C., "Behavior-Based Formation Control for Multirobot Teams," *IEEE Transactions on Robotics and Automation*, Vol. 14, No. 6, 1998, pp. 926–939.

[3]Lewis, M. A., and Tan, K.-H., "High Precision Formation Control of Mobile Robots Using Virtual Structures," *Autonomous Robots*, Vol. 4, Oct. 1997, pp. 387–403.

[4]Sugar, T., and Kumar, V., "Decentralized Control of Cooperating Mobile Manipulators," *Proceedings of the IEEE International Conference on Robotics and Automation*, IEEE Press, Piscataway, NJ, 1998, pp. 2916–2921.

[5]Ogren, P., Fiorelli, E., and Leonard, N. E., "Formations with a Mission: Stable Coordination of Vehicle Group Maneuvers," *15th International Symposium on Mathematical Theory of Networks and Systems*, Center for the Study of Biocomplexity, University of Notre Dame, Notre Dame, IN, 2002.

[6]Tanner, H. G., Pappas, G. J., and Kumar, V., "Input-to-State Stability on Formation Graphs," *Proceedings of the IEEE Conference on Decision and Control*, IEEE Press, Piscataway, NJ, 2002, pp. 2439–2444.

[7]Fierro, R., Das, A., Kumar, V., and Ostrowski, J., "Hybrid Control of Formations of Robots," *Proceedings of the IEEE International Conference on Robotics and Automation*, IEEE Press, Piscataway, NJ, 2001, pp. 157–162.

[8]Fax, J. A., and Murray, R. M., "Information Flow and Cooperative Control of Vehicle Formations," *IFAC World Congress*, International Federation of Automatic Control, Laxenburg, Austria, 2002.

[9]Eren, T., Belhumeur, P. N., and Morse, A. S., "Closing Ranks in Vehicle Formations Based on Rigidity," *Proceedings of the IEEE Conference on Decision and Control*, IEEE Press, Piscataway, NJ, 2002, pp. 2959–2964.

[10]Ogren, P., Egerstedt, M., and Hu, X., "A Control Lyapunov Function Approach to Multiagent Coordination," *IEEE Transactions on Robotics and Automation*, Vol. 18, No. 5, 2002, pp. 847–851.

[11]Giulietti, F., Pollini, L., and Innocenti, M., "Autonomous Formation Flight," *IEEE Control Systems Magazine*, Vol. 20, No. 6, 2000, pp. 34–44.

[12]Stilwell, D. J., and Bishop, B. E., "Platoons of Underwater Vehicles," *IEEE Control Systems Magazine*, Vol. 20, No. 6, 2000, pp. 45–52.

[13]Kang, W., and Yeh, H.-H., "Co-Ordinated Attitude Control of Multi-Satellite Systems," *International Journal of Robust and Nonlinear Control*, No. 12, 2002, pp. 185–205.

[14]Carpenter, J. R., "Decentralized Control of Satellite Formations," *International Journal of Robust and Nonlinear Control*, No. 12, 2002, pp. 141–161.

[15]Anderson, M. R., and Robbins, A. C., "Formation Flight as a Cooperative Game," *Proceedings of the AIAA Guidance, Navigation and Control Conference*, AIAA, Reston, VA, 1998, pp. 244–251.

[16]Wang, P. K. C., and Hadaegh, F. Y., "Coordination and Control of Multiple Microspacecraft Moving in Formation," *The Journal of the Astronautical Sciences*, Vol. 44, No. 3, 1996, pp. 315–355.

[17]Hadaegh, F. Y., Lu, W.-M., and Wang, P. K. C., "Adaptive Control of Formation Flying Spacecraft for Interferometry," IFAC, 1998.

[18]Robertson, A., Inalhan, G., and How, J. P., "Formation Control Strategies for a Separated Spacecraft Interferometer," *Proceedings of the American Control Conference* (San Diego), American Automatic Control Council, Evanston, IL, 1999.

[19]Mesbahi, M., and Hadaegh, F. Y., "Formation Flying Control of Multiple Spacecraft via Graphs, Matrix Inequalities, and Switching," *Journal of Guidance, Control, and Dynamics*, Vol. 24, No. 2, 2000, pp. 369–377.

[20]Wie, B., Weiss, H., and Apapostathis, A., "Quaternion Feedback Regulator for Spacecraft Eigenaxis Rotations," *Journal of Guidance, Control, and Dynamics*, Vol. 12, No. 3, 1989, pp. 375–380.

[21]Beard, R. W., McLain, T. W., Goodrich, M., and Anderson, E. P., "Coordinated Target Assignment and Intercept for Unmanned Air Vehicles," *IEEE Transactions on Robotics and Automation*, Vol. 18, No. 6, 2002, pp. 911–922.

[22]Leonard, N. E., and Fiorelli, E., "Virtual Leaders, Artificial Potentials and Coordinated Control of Groups," *Proceedings of the IEEE Conference on Decision and Control*, IEEE Press, Piscataway, NJ, 2001, pp. 2968–2973.

[23]Beard, R. W., Lawton, J., and Hadaegh, F. Y., "A Coordination Architecture for Formation Control," *IEEE Transactions on Control Systems Technology*, Vol. 9, No. 6, 2001, pp. 777–790.

[24]Young, B., Beard, R., and Kelsey, J., "A Control Scheme for Improving Multi-Vehicle Formation Maneuvers," *Proceedings of the American Control Conference* (Arlington, VA), American Automatic Control Council, Evanston, IL, 2001.

[25]Ren, W., and Beard, R. W., "Virtual Structure Based Spacecraft Formation Control with Formation Feedback," AIAA Paper 2002-4963, Aug. 2002.

[26]Lawton, J., Young, B., and Beard, R., "A Decentralized Approach to Elementary Formation Maneuvers," *IEEE Transactions on Robotics and Automation* (to be published).

[27]Lawton, J., and Beard, R. W., "Synchronized Multiple Spacecraft Rotations," *Automatica*, Vol. 38, No. 8, 2000, pp. 1359–1364.

[28]Wertz, J. R. (ed.), *Spacecraft Attitude Determination and Control*, Kluwer Academic, Norwell, MA, 1978.

[29]Hughes, P. C., *Spacecraft Attitude Dynamics*, Wiley, 1986.

[30]Wen, J. T.-Y., and Kreutz-Delgado, K., "The Attitude Control Problem," *IEEE Transactions on Automatic Control*, Vol. 36, No. 10, 1991, pp. 1148–1162.

[31]Graham, A., *Kronecker Products and Matrix Calculus: with Applications*, Halsted Press, 1981.